SJSLP

Scientific Journal SLP. Vol 2008 Article 1SJ, 7 pages

Scientific Journal SLP

Lattice vibration calculation of lanthanum hexaferrite

Yu. M. Chumakov[1], S. A. Palomares-Sánchez[2], A. L. Guerrero-Serrano[2,3], and J.R. Martínez[2]

[1]Institute of Applied Physics of Academy of Sciences of Moldova, Kishinev, Moldova. (chumakov.xray@phys.asm.md)
[2]Facultad de Ciencias, Universidad Autónoma de San Luis Potosí, 78000 San Luis Potosí, S.L.P., México.
[3]Centro de Investigación en Materiales Avanzados, Chihuahua, Chih. México.

ARTICLE INFO

Received 8 April 2008
Revised 20 May 2008
Accepted 30 August 2008

KEYWORDS

Electronic properties
Pseudopotentials
Vibrational modes
Magnetic ceramics

ABSTRACT

The electronic properties of lanthanum hexaferrite (La-M) were studied using the density functional theory (DFT) based on pseudopotentials and numerical localized atomic orbitals as basis sets. The calculations were performed using two approximations to DFT, namely, the local density approximation (LDA) and the generalized gradient approximation (GGA), both in the spin-polarized version. For LDA we used the Ceperley-Alder exchange-correlation potential, whereas for the GGA calculations we used the Perdew-Burke-Ernzerhof (PBE) scheme. With these approximations it was found that the lanthanum hexaferrite is metallic with conduction in the majority and minority spin channels. The vibrational analysis of the La-M is reported; the calculations were performed using commercial versions of the density functional programs DMol^3 and the result were compared with those of the Ba hexaferrite (Ba-M).

Introduction

M-type hexaferrites ($MFe_{12}O_{19}$) are technologically important due to their multiple applications as permanent magnets. Most of the research activity in this kind of materials has been devoted to study the properties of Ba, Sr and Pb hexaferrites [1] due to the difficulty to prepare La M-type hexaferrite (La-M) [2]. The study of the magnetic properties of La-M is important because it displays an increase in the magnetocrystalline anisotropy at low temperatures without decrease the magnetization [3].

Recently, La-M has been a subject of continuous interest and intensive experimental work and theoretical study as pure hexaferrite and as La substituted hexaferrite ($La_xSr_{1-x}Fe_{12}O_{19}$). The electronic structure of $La_xSr_{1-x}Fe_{12}O_{19}$ (x = 0, 0.25, 0.5, 0.75, 1) was calculated by the density functional theory and generalized gradient approximation (GGA+U method) using the full potential linearized augmented plane wave (FPLAPW) method with the dual basis set. The ‘virtual crystal’ approach was employed for the fractional x, its applicability was checked for x = 0.5 by comparing it with the supercell method [4]. All calculations were performed with the Gorter spin structure [5] and crystal structure parameters which were identical to $SrFe_{12}O_{19}$ [6] because the structure of La-M has been not reported when we began with the calculations.

In the present work, the Parrinello-Rahman-constant-pressure molecular-dynamics technique was used with variable cell shape [7] as provided within SIESTA code [8] to predict the crystal structure of the lanthanum hexaferrite. In our model, the Sr atom was replaced by La in the $SrFe_{12}O_{19}$ cell [9]. The hydrostatics pressure in the calculations was ranged at room temperature from 0 to 100 GPa. The dependences of total energy and cell volume versus the pressure, as well as the structural changes under pressure, are also calculated and compared with the original $SrFe_{12}O_{19}$ cell. The electronic properties and vibrational spectrum of lanthanum hexaferrite were calculated on the base of found crystal structure of the La-M.

Method

Figures 1 (a)-(b) show the dependence of the structure as a function of the pressure. It was found that there are no major changes up to 100 GPa therefore it is very likely that the structural properties of La-M at 0 GPa remain even under pressure. In this connection, we choose the crystal structure parameters of lanthanum hexaferrite obtained after molecular-dynamics simulation under hydrostatic pressure of 5 GPa in order to investigate its electronic structure.

We have performed density functional theory (DFT) [10, 11] calculations using the SIESTA method [8], which is based on pseudopotentials and numerical localized atomic orbitals as basis sets. The calculations were performed using two approximations to DFT, namely, the local density approximation (LDA) [12] and the generalized gradient approximation (GGA) [13], both in the spin-polarized version with spins on 2a, 2b and 12k Fe sites antiparallel to spins on 4f1 and 4f2 Fe sites as it was found to have the lowest total energy in the experimentally observed stable Gorter’s structure [5] for strontium hexaferrite [6]. For LDA we used the Ceperley-Alder exchange-correlation potential [14] whereas for the GGA calculations we used the Perdew-Burke-Ernzerhof (PBE) scheme [13].

Core electrons were replaced by norm-conserving pseudopotentials using the scalar-relativistic Troullier-Martins scheme [15] in the Kleinman-Bylander factorised form [16] with nonlinear core corrections [17]. The $5s^2$ $5p^6$ $5d^0$ $4f^0$ and $4s^0$ $4p^0$ $3d^5$ $4f^0$ configurations were used as reference for La and Fe, respectively. Notice that the $5s^2$ and $5p^6$ semicore states of La are explicitly included in the calculations. The core radii for the *s*, *p*, *d* and *f* components of the pseudopotential are 1.85, 2.20, 3.10, 1.40 bohr for La, with a radius for the core correction (rp_c) of 1.50 Bohr. The radii for Fe are 2.0 bohr for all shells with $rp_c = 0.70$ Bohr. For oxygen, we used the pseudopotential from the SIESTA database. All used pseudopotentials were tested by *pt.sh* script from the SIESTA program package. The basis set consists of strictly localized atomic orbitals at the double-ζ polarized level [18].

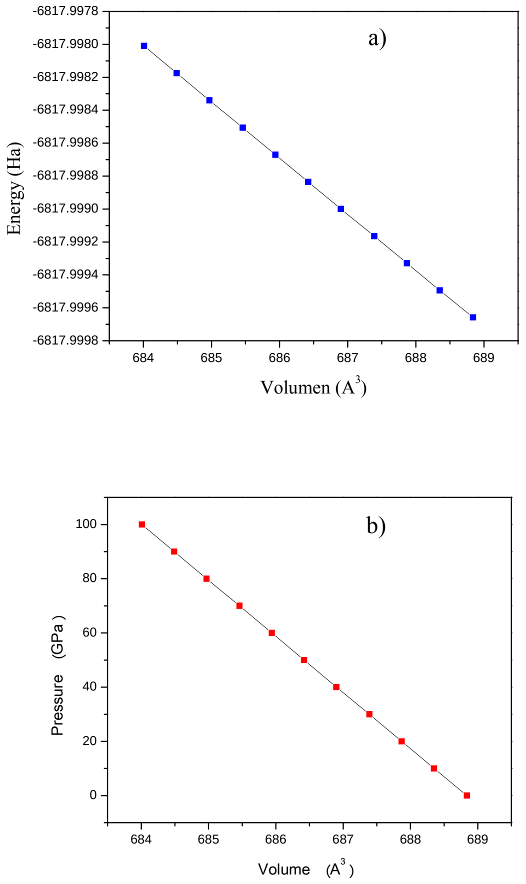

Figure 1. The dependences of energy (a) and volume *versus* the volume under pressure which ranges from 0 to 100 GPa.

Results

The calculated total density of states (DOS) near the Fermi level (which is set at the top of the valence band, $E_F = 0$) and partial density of states (PDOS) of every Fe atom in the Gorter's form of La-M for LDA approximation are shown in figures 2 and 3, respectively. The valence band, which is composed of mainly O 2*p* and Fe 3*d* states, has a total width of about 8.0 eV. The lower part (from about −7.8 to −3.9 eV) is dominated by the O 2*p* character, while the upper part (from about −3.9 eV to the Fermi level) is mainly composed of Fe 3*d* character hybridized with some O 2*p* states. The calculations show that O 2*p* and Fe 3*d* states are dominated at the bottom of the conduction band. The crystal field splittings (doublet e_g and triplet t_{2g}) were not observed for the octahedral Fe atoms on the 2*a*, $4f_2$ and 2*k* sites as well as for tetrahedral Fe at $4f_1$ and bipyramidal Fe at 2*b* positions due to hybridization with some O 2*p* states and the super-exchange interactions between the Fe ion at 2*b* and those at 12*k*.

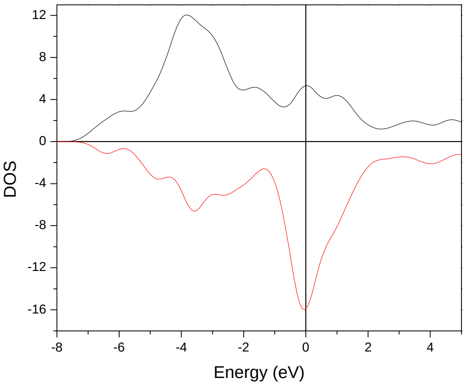

Figure 2. Total DOS of La-M with Gorter's form for LDA approximation

The figure 4 shows the dispersion curves along the high symmetry lines in the Brillouin zone (BZ) for the spin-up (a) and spin-down (b) electrons of the Gorter's form of MLa. They show a strong anisotropy with rather strong dispersion along the directions perpendicular to the c axis (*Γ–H*, *Γ–M*, *Γ–L* and *A–L*) and very small dispersions along the directions parallel to the c axis (*Γ–A*, *K–H* and *M–L*). Thus, with the LDA approximation we found that the lanthanum hexaferrite is metallic with conduction in the majority and minority spin channels. The use of the generalized gradient approximation led to the same result.

The total DOS and PDOS for the Fe ions of La-M with Gorter's form for GGA approximation, as well as the dispersion curves along the high symmetry lines in the BZ, are presented on figures 5-7. The valence band, which is composed of mainly O 2*p* and Fe 3*d* states, has a total width of about 6.0 eV. The lower part (from about −6.0 to −4.5 eV) is dominated by O 2*p* character, while the upper part (from about −4.5 eV to the Fermi level) is mainly composed of Fe

$3d$ character hybridized with some O $2p$ states. The calculations show that O $2p$ and Fe $3d$ states are dominated at the bottom of conductivity band. The crystal field splittings (doublet e_g and triplet t_{2g}) were not observed for the octahedral Fe atoms on $2a$, $4f_2$ and $2k$ sites as well as for tetrahedral Fe at $4f_1$ and bipyramidal Fe at $2b$ positions due to hybridization with some O $2p$ states and the super-exchange interactions between the Fe ion at $2b$ and those at $12k$. The dispersion curves show a strong anisotropy with rather strong dispersion along the directions perpendicular to the c axis (*Γ–H*, *Γ–M*, *Γ–L* and *A–L*) and very small dispersions along the directions parallel to the c axis (*Γ–A*, *K–H* and *M–L*).

Thus, with the LDA approximation we found that the lanthanum hexaferrite is metallic with conduction in the majority and minority spin channels. The use of the generalized gradient approximation led to the same result.

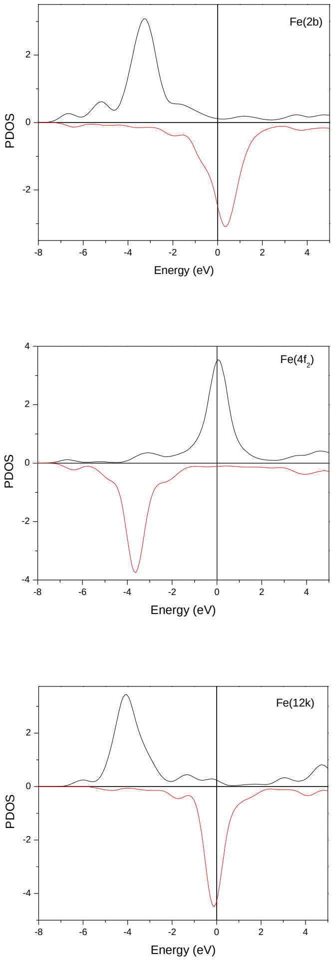

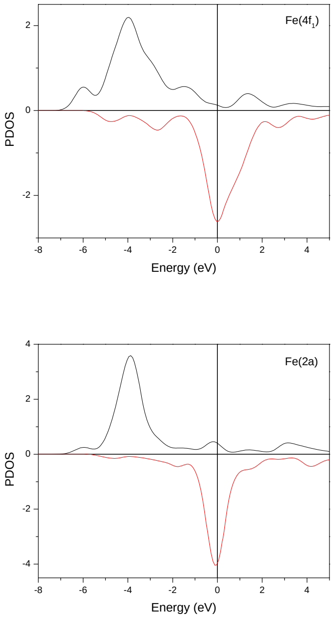

Figure 3. Partial density of states (PDOS) of Fe ions of La-M with Gorter's form for LDA approximation.

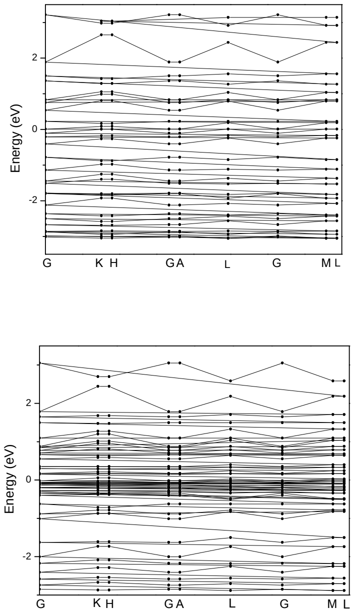

Figure 4. Dispersion curves along the high symmetry lines in the BZ of La-M with Gorter's form for the spin-up (a) and spin-down (b) electrons for LDA approximation.

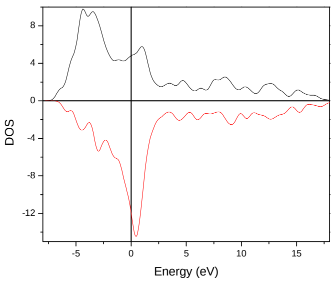

Figure 5. Total DOS of La-M with Gorter's form for GGA approximation.

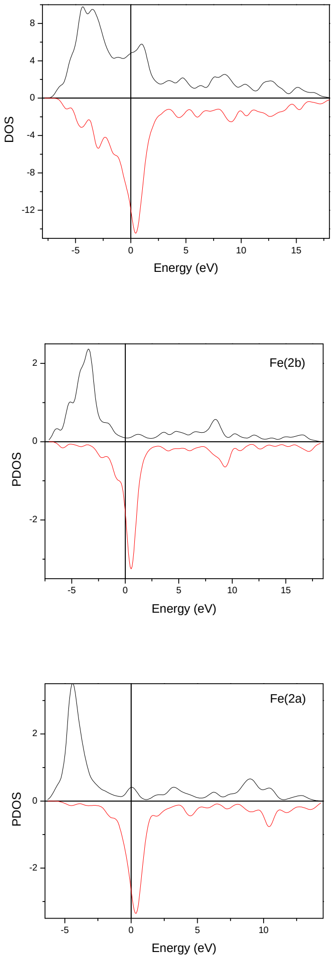

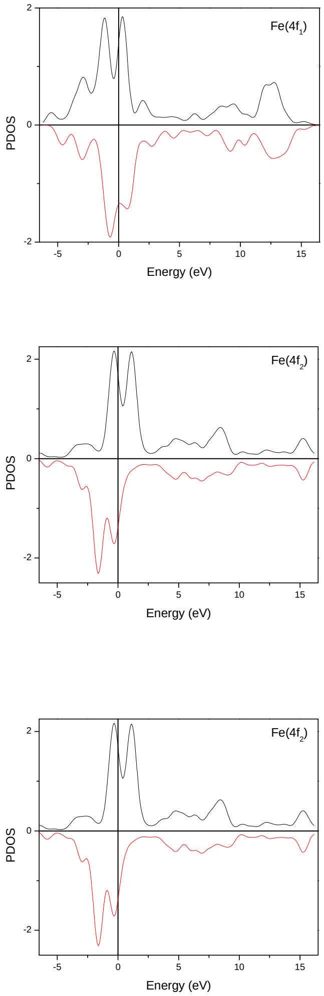

Figure 6. Partial density of states (PDOS) of Fe ions of hexaferrite $LaFe_{12}O_{19}$ with Gorter's form for GGA approximations.

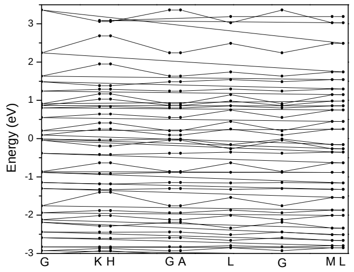

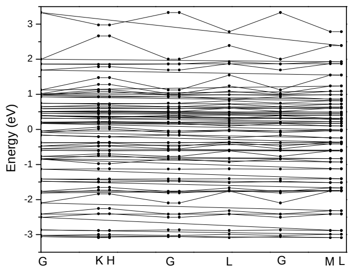

Figure 7. Dispersion curves along the high symmetry lines in the BZ of La-M with Gorter's form for the spin-up (a) and spin-down (b) electrons for GGA approximation.

In [2] it was shown that all mixed valence compounds including the stoichiometric $LaFe_{12}O_{19}$ are half-metals with conduction in the minority spin channel.

In order to study the vibrational properties of La-M the supercell, containing of 64 atoms, it has been constructed as proposed in [19], where the first Raman spectra of barium hexaferrite were reported. The compounds of La-M and $BaFe_{12}O_{19}$ are practically isostructural [20]; therefore, the crystal structure of lanthanum hexaferrite consists of a close-packed stacking of oxygen or lanthanum-oxygen layers, and the iron atoms are distributed within three kinds of octahedral sites, one tetrahedral site, and one bipyramid site, figure 8.

The structure is usually described in terms of two structural blocks: the spinel block S $(Fe_{11}O_{16})^+$, separated by $(LaFeO_3)$ layers (block R).

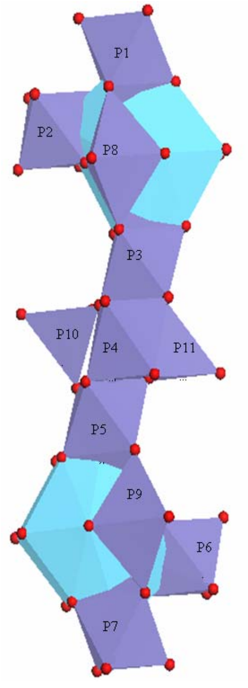

Figure 8. Polyhedra of the La-M crystal structure. P1-P7 are octahedral sites; P8-P9 are tetrahedral sites; P10-P11 are tetrahedral sites of iron atoms.

In [19], it was shown that the 64 atoms in the unit cell give rise to 189 ($k = 0$) optical modes which can be characterized according to the D_{6h} factor group of the crystal by using group theoretical methods. It was found that, based on D_{6h} symmetry, 42 Raman-active modes $(11A_{1g}+14E_{1g}+17E_{2g})$ and 30 IR-active modes $(13A_{2u}+17E_{1u})$ are expected. The other optical modes are silent modes $(3A_{1u}+4A_{2g}+13B_{1g}+4B_{1u}+3B_{2g}+12B_{2u}+15E_{2u})$. One A_{2u} mode and one doubly degenerate E_{1u} mode correspond to acoustic modes.

The vibrational analysis of $LaFe_{12}O_{19}$ was done by finite differences and all calculations were performed using commercial versions of the density functional programs DMol3 [21], available from Molecular Simulations Inc. The finite difference approach directly calculates the force constants matrix from first principles [22, 23, 24]. In this method a single atom is displaced successively in the x, y, and z direction and the forces on all atoms in the unit cell are calculated from the Hellmann-Feynman theorem [25]. To account for anharmonic effects a negative and a positive displacement is done for all three direction (the force constants are averaged for positive and negative displacement), which means a total of 6 self-consistent cycles per atom. Then the next atom is displaced until the force constant matrix is complete. The dynamical matrix is set up and diagonalized yielding all phonon frequencies and eigenvectors [21]. The frequencies of the Raman bands observed at room temperature for $BaFe_{12}O_{19}$ and calculated ones for $LaFe_{12}O_{19}$ are listed along with the appropriate symmetry assignments in Table 1. There is a good agreement between the calculated vibrational frequencies for La-M and observed ones for $BaFe_{12}O_{19}$ because the root-mean-square (RMS) for given modes is equal to 2 cm^{-1} and this value usually ranges from 17 to 20 cm-1 [26]. The RMS is calculated as $[(\Sigma^{N}_{i=1}(\Delta\nu_i)^2/N]^2$, where N is number of normal modes and $\Delta\nu_i$ is the difference between a calculated and measured frequency. The description of the vibrations for observed Raman frequencies of 216, 453, 684 and 713 cm^{-1} for $BaFe_{12}O_{19}$ coincide with calculated ones for La-M, Table 1. In particular, the symmetric stretching mode of the bipyramidal Fe(2)O5 group in $LaFe_{12}O_{19}$, characteristic of the M-hexaferrite structure, has been found to be responsible for the strongest Raman band at 685.91 cm^{-1} [19]. The difference in description of Raman bands in $BaFe_{12}O_{19}$ and La-M occurs for frequencies of 172, 184, 340 and 409 cm^{-1}. In $BaFe_{12}O_{19}$ these modes are associated by spinel block vibrations, mixed octahedral, octahedral Fe_5O_6 polyhedron vibrations, while for $LaFe_{12}O_{19}$ the corresponding modes are characterized by S and R blocks vibrations, octahedral Fe_5O_6 polyhedra, octahedra and Fe_3O_4 tetrahedra vibrations. The above mentioned differences may be cause by mass effect due to replacing the Ba atom by La one.

Nominally the peaks corresponding to 172, 184, 340, and 409 cm^{-1} are convoluted in the Raman spectra for the Ba-M ferrite. In samples prepared with excessive Fe^{3+}, they occupy the octahedron interstices similar to the FeO_6 octahedron at the 12k site and the bipyramid interstices similar to the FeO_5 bipyramid at the 2*b* site, as the Fe concentration is increased. The percentage of integral intensity for the Raman bands at 412 and 336 cm^{-1} gradually increased with excessive Fe^{3+} and decreased remarkably when the Fe^{3+} concentration growth at 0.4 [27].

Thus, the vibrational analysis of $LaFe_{12}O_{19}$ showed the good agreement between the calculated vibrational frequencies for La-M and observed ones for $BaFe_{12}O_{19}$ as well as the coincidence of description of the vibrations for observed Raman frequencies of 216, 453, 684 and 713 cm^{-1}. The found difference in description of Raman bands in $BaFe_{12}O_{19}$ and $LaFe_{12}O_{19}$ for frequencies of 172, 184, 340 and 409 cm^{-1} may referred to mass effect caused by replacing a Ba atom by a La one.

ACKNOWLEDGMENTS

The authors wish to thank the financial support of the Programa de Mejoramiento para el Profesorado (PROMEP) under contract PROMEP/103.5/04/1386, México.

Table 1. Comparison between the Raman spectra of $BaFe_{12}O_{19}$ and $LaFe_{12}O_{19}$.

$BaFe_{12}O_{19}$			$LaFe_{12}O_{19}$	
Frequency (cm^{-1})	^{a}[19]	Description	Frequency (cm^{-}1)	Description
173	E1g	Whole spinel block	175.44	S + R blocks
184	E1g	Whole spinel block	186.33	S + R blocks
208	E2g		202.72	
212	E1g		211.09	
215	E1g		214.10	
216	A1g	O-Fe-O bridge	218.78	O-Fe-O bridge
250	E1g		249.26	
285	E1g		281.82	
317	A1g		317.88	
319	E2g		321.32	
317	E1g		317.88	
335	E2g		334.54	
340	A1g	Octahedra (mixed)	342.26	Octahedra FeO_6 and Fe_5O_6
340	E1g		-	
385	E2g		384.25	
409	A1g	Fe_5O_6 octahedra dominated	411.39	octahedra and Fe_3O_4
417	E1g		417.41	
420	E2g		422.80	
451	E1g		449.36	
453	A1g	Octahedra FeO_6 and Fe_5O_6	456.00	Octahedra FeO_6 and Fe_5O_6
512	A1g		512.39	
527	E1g		526.79	
529	E2g		534.94	
566	E2g		566.00	
606	E2g		604.23	
609	E1g		609.91	
611	E1g	Octahedra (mixed)	-	
612	E2g		613.31	Octahedra Fe_4O_6 and Fe5O6
614	A1g	Octahedra Fe_4O_6	-	
684	A1g	Bipyramid Fe_2O_5	685.91	Bipyramid Fe_2O_5
713	A1g	Tetrahedra Fe_3O_4	712.27	Tetrahedra Fe_3O_4

[a] Symmetry assignment based on the analysis of the observed Raman tensors in [19].

REFERENCES

1. H. Kojima. *Ferromagnetic Materials*, edited by E.P. Wolfarth (North-Holland, Amsterdam, 1982), Vol. 3.
2. M. Kupferling, R. Grossinger, V. Corral-Flores, J. Matutes-Aquino. J. Mag. Mag. Mater. 290-291 (2005) 1255.
3. F. K. Lotgering, J. Phys. Chem. Solids 35 (1974) 1633.
4. P. Novák, K. Knižek, M. Küpferling, R. Grössinger, M. W. Pieper. Eur. Phys. J. B 43 (2005) 509.
5. E. W. Gorter, Proc. IEEE 104B (1957) 255.
6. C. M. Fang, F. Kools, R. Metselaar, G. de With, R. A. de Groot, J. Phys: Condens. Matter 15 (2003) 6229.
7. M. Parrinello, A.Rahman, Phys. Rev. Lett. 45 (1980)1196.
8. J. M. Soler, E. Artacho, J. D. Gale, A. García, J. Junquera, P. Ordejón, D. Sánchez-Portal, J. Phys.: Condens. Matter 14 (2002) 2745.
9. X. Obradors, X. Solans, A. Collomb, D. Samaras, J. Rodrígues, M. Pernet, M. Font-Altaba. 72 (1988) 218.
10. P. Hohenberg, W. Kohn, Phys. Rev. B (1964) 864.
11. W. Kohn and L. J. Sham, Phys. Rev. (1965) A1133–A1138.
12. J. P. Perdew, A. Zunger, Phys. Rev. B 23 (1981) 5048.
13. J. P. Perdew, K. Burke, M. Ernzerhof, Phys. Rev. Lett. (1996) 3865.
14. D. M. Ceperley, B. J. Alder, Phys. Rev. Lett. 45 (1980) 566.
15. N. Troullier, J. L. Martins, Phys. Rev. B 43, 1993 (1991).
16. L. Kleinman, D. M. Bylander, Phys. Rev. Lett. 48 (1982) 1425.
17. S. G. Louie, S. Froyen, M. L. Cohen, Phys. Rev. B 26 (1982) 1738.
18. E. Artacho, D. Sánchez-Portal, P. Ordejón, A. García, J.M. Soler, Phys. Stat. Sol. (b) (1999) 809.
19. J. Kreisel, G. Lucazeau, H. Vincent. Journal Sol. State Chem. 137 (1998) 127.
20. A. Collomb, P. Wolfers, X. Obradors. J. Mag. Mag. Mater.63 (1986) 57.
21. (a) B. Delley, J. Chem. Phys. 92 (1990) 508; (b) B. Delley, J. Schefer, T. Woike, ibid. 107 (1997) 10067; (c) A. Kessi, B. Delley, Int. J. Quantum Chem. 68 (1998) 135.
22. D. Sánchez-Portal, E. Artacho, J. M. Soler, A. Rubio, P. Ordejon. Phys. Rev. B 59 (1999) 12678.
23. P. Ordejon, E. Artacho, J. M. Soler. Phys. Rev. B 53 (1996) R10 441.
24. W. Frank, C. Elsässer, M. Fhnle, Phys. Rev. Lett. 74 (1995) 1791.
25. R. P. Feynman. Phys. Rev. 56 (1939) 340.
26. V. Brazdova, M. V. Ganduglia-Pirovano, J. Sauer. J. Phys. Chem., B 105, (2005) 394.
27. W. Y. Zhao, P. Wei, X. Y. Wu, W. Wang, and Q. J. Zhang, J Appl. Phys. 103, (2008) 063902